ILASS Americas, 17th Annual Conference on Liquid Atomization and Spray Systems, Arlington, VA, May 2004

Effect of Surface Thermal Variations during Cryogen Spray Cooling in Dermatologic Laser Therapy

W. Franco[1], G. X. Wang[2], E. Karapetian[3, 4], J. S. Nelson[4] and G. Aguilar[1*]
[1]Department of Mechanical Engineering, University of California, Riverside, CA 92521
[2]Department of Mechanical Engineering, University of Akron, Akron, OH 44325
[3]Department of Chemical Engineering and Materials Science, University of California, Irvine, CA 92612
[4]Beckman Laser Institute, University of California, Irvine, CA 92612

Abstract

Cryogen spray cooling (CSC) is a spatially selective heat transfer technique that provides epidermal protection during laser treatment of selected dermatoses, such as port wine stain (PWS) birthmarks. Most numerical studies of CSC-assisted PWS therapies to date assume constant cooling conditions at the skin surface. In the present study, however, we show that cooling conditions at the skin surface vary significantly both in time and space. The objective of this paper is to assess the effect of thermal variations at the skin surface on the heat extraction process during PWS laser therapy. First, a single temperature sensor systematically recorded temperature changes along the sprayed area of a skin model. Next, a multiple temperature sensor acquired temperature data at four strategic radial locations namely, at the center, middle, perimeter and outside the sprayed area. Finally, recorded temperatures along with an inverse heat conduction problem (IHCP) algorithm were used to study the heat extraction process at the surface. Spatial and dynamic profiles of surface temperatures, heat fluxes, heat transfer coefficients and heat removal are presented. Results show that local and temporal variations of the boundary conditions may have a strong influence on CSC cooling efficiency during dermatologic laser therapy. The study shows that external conditions must be considered and ideally controlled to optimize current laser therapies of selected dermatoses, such as PWS.

Introduction

Cooling and heating processes are essential to many medical treatments, such as laser therapy of dermatologic vascular lesions, basal skin carcinomas and cartilage reshaping for reconstructive surgery. Port wine stain (PWS) is a congenital and progressive vascular malformation of the dermis. Laser irradiation at appropriate wavelengths induces permanent thermal damage to PWS blood vessels. However, laser energy is also absorbed by epidermal melanin causing localized heating therein. As a consequence, complications such as hypertrophic scarring and skin dyspigmentation may occur. Cryogen spray cooling (CSC) is a spatially selective heat transfer technique that spurts liquid cryogen onto the skin surface. The cryogen evaporates extracting heat from the epidermis thereby increasing the threshold for epidermal damage [1].

Heat transferred through the skin surface during CSC is a function of many fundamental spray parameters [2, 3] that vary in time and space within the spray cone (average droplet diameter and velocity, mass flow rate, temperature and spray density). Therefore, a non uniform surface heat flux at the skin surface occurs during CSC-assisted dermatologic laser treatment. During CSC, uniform cooling within the sprayed area is highly desirable but not practical. Despite surface variations, most numerical studies on CSC-assisted PWS therapy to date assumed constant heat transfer conditions at the skin surface.

In the present study, the effect of surface thermal variations during CSC is experimentally and numerically addressed. First, a single temperature sensor was used to measure temporal and radial temperature values along the radius of the sprayed surface of a skin model. Next, a multiple temperature sensor was used to measure temperatures values at four specific radial locations on the skin model namely, three within and one outside the sprayed surface. Finally, an inverse heat conduction problem (IHCP) algorithm was applied to determine the temperature, heat flux, heat transfer coefficient and total heat removal at the surface of the skin model.

Experimental and Numerical Methods

In this section, only a brief description of the materials and experimental and numerical methods is presented. A more detailed description of the temperature sensors and computer algorithm can be found in the referenced literature.

Cryogen spray system

Cryogen R-134a (1, 1, 1, 2-tetrafluoroethane) was delivered through a high pressure hose to a fuel injector

*Corresponding author

attached to a straight-tube-nozzle. R-134a, (with a boiling temperature at atmospheric pressure of T_b≈26 °C) was kept at saturation pressure (600 kPa at 25 °C). A nozzle with an inner diameter d_1=0.7 mm and length l_1=63.6 mm was used for the single temperature sensor. A nozzle with d_2=0.57 mm and l_2=8 mm was used for the multiple temperature sensor. The spray characteristics produced by these and other nozzles have previously been reported [4, 5]. Nozzle length has little influence on spray characteristics. However, nozzle diameter choice, on the other hand, has a dramatic effect on spray characteristics [4, 6]. Nozzles can be classified as narrow (0.5≤d≤0.8 mm) and wide (d≈1.4 mm) based on spray characteristics [6]. Therefore, the two nozzles employed in this study are classified as narrow with equivalent cryogen spray characteristics.

Temperature sensors

The first measuring device employed a single temperature sensor as schematically shown in Fig. 1(a). A miniature type-K thermocouple was placed on top of a 12.5 mm square bar of polymethyl methacrylate (Plexiglass®). Cellulose tape (Scotch tape®), 50 µm thick, was placed next to the thermocouple bead. A piece of aluminum foil (15 x 10 mm) covers the sensor. Thermal paste around the thermocouple bead is used to ensure good thermal contact.

The second measuring device employed multiple temperature sensors as schematically shown in Fig. 1(b). The device has four silver disks of 3.18 mm diameter and 0.17 mm thickness. Disks are placed 1 mm apart from each other. The top surface of each disk is exposed to the spray while the lateral and bottom surfaces are embedded in epoxy. Type-K thermocouples are welded to the bottom of each disk.

These temperature sensors provide a substrate that has thermal properties similar to skin such that total heat removal Q, surface heat flux q and heat transfer

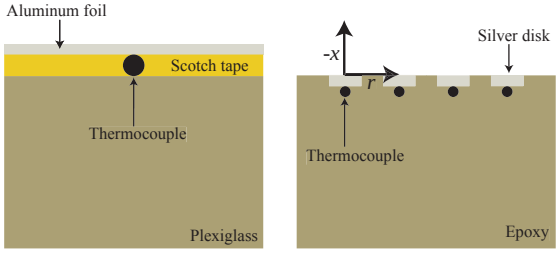

(a) (b)

Figure 1. (a) Single and (b) multiple temperature sensors.

coefficient h are qualitatively similar to those expected for human skin. Thermal properties of human skin, Plexiglass® and epoxy can be found in the literature [7, 8, 9]. The single sensor was used to obtain temperature measurements every 0.5 mm on the area where the cryogen was deposited. The multiple sensors were used to measure temperatures namely, at the center, middle, perimeter and outside the sprayed area.

Heat transfer calculations

A one-dimensional heat conduction algorithm was used to compute the surface heat flux q from temperature measurements. This approximation relies on the fact that the width of the sprayed area (≈ 16 mm) is much larger than the depth (≈ 0.17 mm) of temperature measurements. Indeed, the time scale and depth of relevance in PWS treatment are milliseconds and 0.5 mm, respectively. The applied inverse heat conduction problem (IHCP) algorithm is based on Beck's sequential function specification method [10], where q is estimated as a piecewise constant function of time. A discussion of this algorithm as applied to CSC can be found elsewhere [11].

Experiments

In the first set of experiments, the nozzle located 40 mm from the surface of the single sensor delivered a cryogen spurt of 60 ms. The thermocouple was initially placed at the center of the spray cone (r=0 mm), subsequently, the thermocouple was displaced 0.5 mm from the center. Temperature measurements were recorded every 0.5 mm from r=0 to 7 mm. In the subsequent experiments, the nozzle located 40 mm away from the surface of the multiple temperature sensor delivered a cryogen spurt of 100 ms. The initial skin model temperature in both cases was 22.5 °C.

Results and Discussion

In the presentation of experimental results noise is filtered out by taking a running average using the subsequent and previous five measurements in time.

Four independent runs with the single temperature sensor were performed at every radial location. Figure 2 shows the average values of four independent temperature measurements (T_A) at r=0 mm. The error bars denote standard deviations. Similar curves were obtained for the remaining locations. Three independent runs were performed with the multiple sensor. The standard deviations obtained were similar to those for the single sensor.

Thermal dynamics and radial variations

Temperature measurements, T_m, recorded by the single sensor every 0.5 mm from the center (r=0 mm) to the perimeter (r=7 mm) of the sprayed surface are shown in Fig. 3. The closer to the center of the spray cone the sensor is, the faster the thermal response is and the lower the temperature values are. The temperature

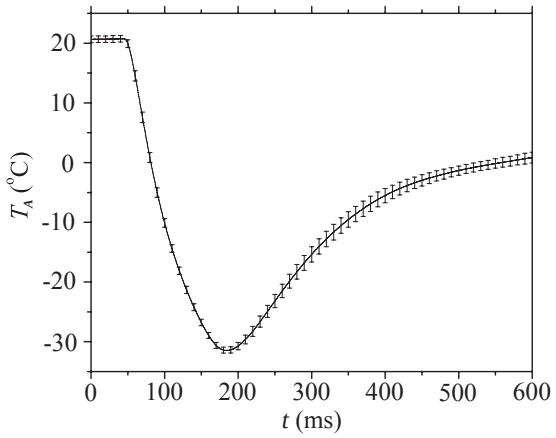

Figure 2. Average measured temperatures for four independent tests. The bars denote standard deviations.

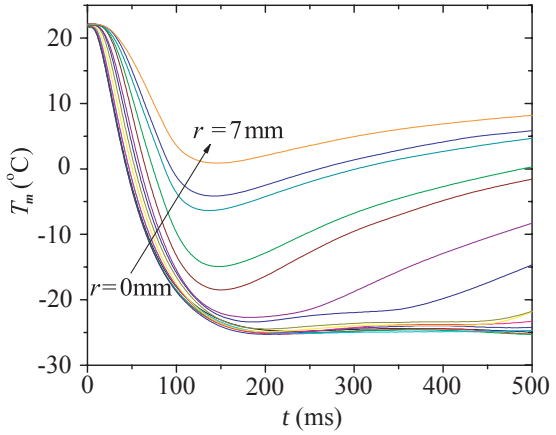

Figure 3. Dynamics of measured temperatures at different radial locations.

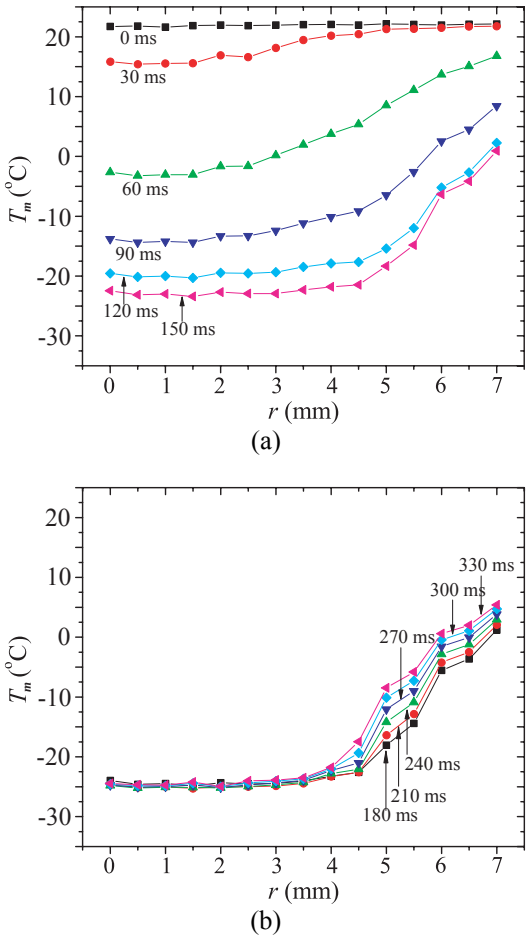

Figure 4. Radial temperature distributions (a) before local minimum temperatures and (b) afterwards.

distribution along the radial direction at specific times is presented in Fig. 4, where curves are plotted every 30 ms. Figure 4(a) shows the radial profile before the center reaches minimum temperature, i.e. T_m for $t \leq 150$ ms. Minimum temperatures are not reached simultaneously. The third curve from the top to the bottom corresponds to the end of the 60 ms spurt. Figure 4(b) shows the radial profile of T_m for $t > 150$ ms. Temperature values are almost the same from the center of the sprayed area up to 4 mm. Thereafter, temperature differences between the center and the perimeter are as great as 20 °C.

Temperatures measured by the multiple sensor along with the IHCP algorithm were used to explore the heat transferred at the surface of the skin model. Dynamics of surface temperature T_s for r=0, 4.18, 8.36 and 12.54 mm are shown in Fig. 5(a). As observed with the single sensor, the closer to the center of the spray cone the sensor is, the faster the thermal response is and the lower temperature values are. At r_4=12.54 mm, the change in temperature is very small since the diameter of the spray cone at the surface is approximately 8 mm. Changes at this location are mainly due to lateral conduction which is small because of the insulator nature of the skin model (that has thermal properties similar to human skin). The phase space T_s-r is plotted in Fig. 5(b). Curves are plotted every 20 ms and the sixth curve from top to bottom corresponds to the end of the 100 ms spurt. There are significant temperature variations along the radial direction. r_1=0 mm and r_3=8.36 mm represent the center and perimeter of the sprayed area, respectively, and r_2=4.18 mm is an intermediate point. Temperature differences among these three locations are initially large but over time they become smaller. However, the differences are significant even when the rate of change is small. The differences in T_s values between the center and perimeter of sprayed area is more than 10 °C for the lowest curve in Fig. 5(b).

The surface heat flux q as a function of time is shown in Fig. 6(a) for r_1, r_2, r_3 and r_4. The closer to the center the sensor is the larger the local maximum heat flux q_{max} is and the sooner it happens. The overall

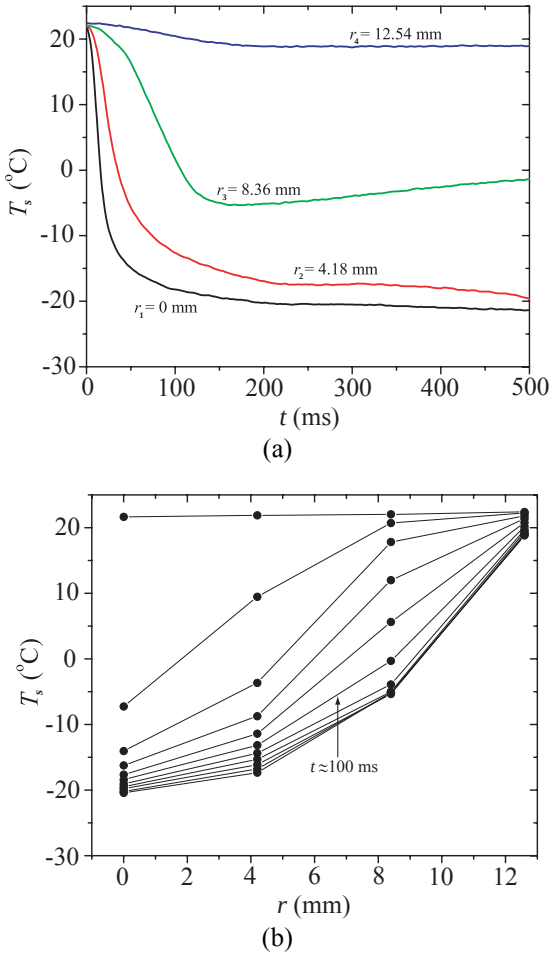

Figure 5. (a) Dynamics and (b) radial distributions of surface temperatures.

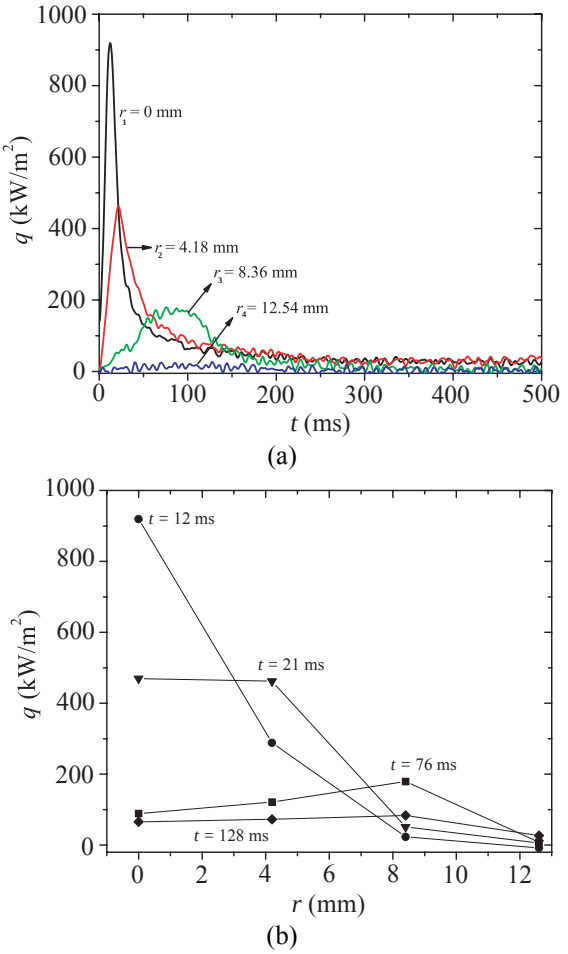

Figure 6. (a) Dynamics and (b) radial distributions of surface heat flux.

maximum heat flux q_c rises at the center of the sprayed area. As expected, at r_4 the surface heat flux is very small since the difference in temperature between the substrate and the environment is also small. The radial profiles for which q is maximal at every location are plotted in Fig. 6(b). Curves correspond to t=12, 21, 76 and 128 ms. $q_{max}(r_1, t)$ is initially the largest, but over time it decreases and $q_{max}(r_2, t)$ becomes largest. Later on, $q_{max}(r_3, t)$ becomes the largest. That is, the peak value $q_{max}(r, t)$ moves from the center to the periphery. The magnitude of the peak value decreases over time.

An average temperature of the cryogen layer T_{cryo}=-56 °C was used to estimate the heat transfer coefficient h [12]. Dynamics of h for all radial locations are shown in Fig 7(a). Radial profiles of h are shown in Fig. 7(b). Curves respectively correspond to the times when local maximum q occurs at each radial location, that is t=12, 21, 76 and 128 ms.

The total heat removal Q was also estimated. Dynamics of Q for all radial locations is shown in Fig. 8(a). The closer to the center of sprayed surface the sensor is the larger the heat removal is. This is true at all times. Figure 8(b) shows radial profiles of Q for the times when local maximal q rises at each radial location.

Conclusions

Single and multiple sensors were used to study the heat transfer dynamics on skin models during CSC.

The single sensor was used to collect temperature data every 0.5 mm on a 7 mm spray from the center of the sprayed surface to the periphery. The difference in temperature values among different locations may be significant, especially between center and peripheral locations. The closer to the center the sensor is the faster the thermal dynamic response is.

Data collected by the multiple sensor was processed by an IHCP algorithm to estimate T_s, q, h and Q as a function of time. The heat transfer process at the surface is a complex temporal and spatial phenomenon. The overall maximum heat flux q_c rises early in time at the center of the sprayed surface. The peak value q_{max}

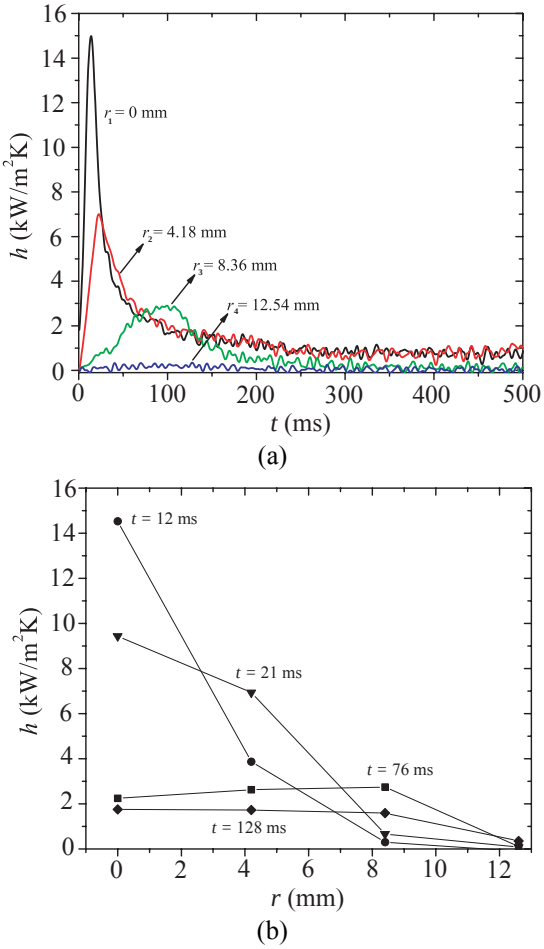

Figure 7. (a) Dynamics and (b) radial distributions of heat transfer coefficient.

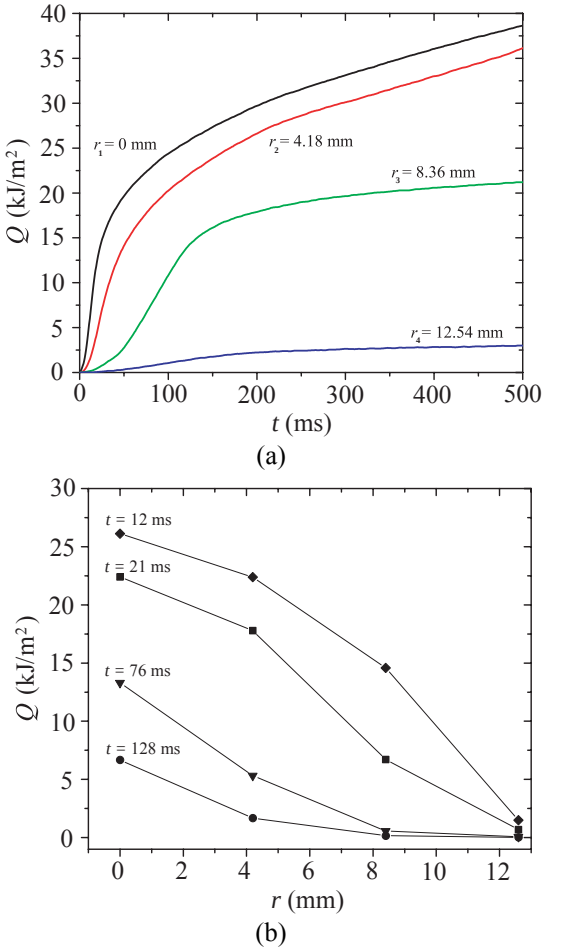

Figure 8. (a) Dynamics and (b) radial distributions of surface heat removal.

moves from the center to the periphery and its magnitude decreases after $q_{max} = q_c$. A similar situation is observed for the heat transfer coefficient; h_{max} changes in time and space. This is not the case for heat removal where at any given time, the closer to the center of the sprayed area the larger Q is, that is Q_{max} always occurs at 0 mm.

Acknowledgements

This work was supported in part by the National Institutes of Health (HD42057 to GA and AR47551, AR48458 and GM62177 to JSN).

Nomenclature

d	nozzle diameter (mm)
h	heat transfer coefficient (kW/m^2 K)
l	nozzle length (mm)
q	surface heat flux (KW/m^2)
Q	heat removal (KJ/m^2)
r	radial coordinate (mm)
T	temperature (°C)
t	time (ms)

Subscripts

A	average
b	boiling
c	overall maximum
cryo	cryogen
m	measured
max	local maximum
s	surface

References

1. J.S. Nelson, T.E. Milner, B. Anvari, B.S. Tanenbaum, S. Kimel, L.O. Svaasand, S.L. Jacques, *Arch. Dermatol.*, 131: 695-700 (1995).
2. G. Aguilar, B. Majaron, W. Verkryusse, Y. Zhou, J.S. Nelson and E.J. Lavernia, *Int. J. Heat Mass Transfer*, 44: 3201-3211 (2001).

3. G. Aguilar, B. Majaron, K. Pope, L.O. Svaasand, E.J. Lavernia and J.S. Nelson, *Lasers Surg. Med.*, 28: 113-20 (2001).
4. E. Karapetian, *Influence of cryogenic spray parameters on surface heat extraction on human skin*, Master's thesis, University of California, Irvine, California (2002).
5. G. Aguilar, G.X. Wang and J.S. Nelson, *Lasers Surg. Med.*, 32: 152-159 (2003).
6. G. Aguilar, B. Majaron, E. Karapetian, E.J. Lavernia and J.S. Nelson, *IEEE Trans. Biomed. Eng.*, 50 (7): 863-869 (2003).
7. F.A. Duck, *Physical properties of tissue*, London, Academic press 1990.
8. G. Aguilar, S.H. Diaz, E.J. Lavernia and J.S. Nelson, *Lasers Surg. Med.*, 31: 27-35 (2002).
9. G. Aguilar, G.X. Wang and J.S. Nelson, *Phys. Med. Biol.*, 48: 2169-2181 (2003).
10. J. V. Beck and B. Blackwell and C. R. St Clair, *Inverse heat conduction: Ill posed problems*, New York, Wiley, 1990.
11. J.W. Tunnel and J.H. Torres and B. Anvari, *Ann. Biomed. Eng*., 30: 19-33 (2002).
12. G. Aguilar, W. Verkryusse, B. Majaron, L.O. Svaasand, E.J. Lavernia and J.S. Nelson, *IEEE J. Sel. Top. Quantum Electron*, 7: 1013-1021 (2001).